

# Experimental and theoretical behaviour analysis of steel suspension members subjected to tension and bending

Stanislav Kmet\*, Michal Tomko and Molinne Bin

*Faculty of Civil Engineering, Technical University of Kosice, Vysokoskolska 4, 042 00 Kosice, Slovakia*  
(Received December 23, 2011, Revised April 13, 2012, Accepted July 24, 2012)

**Abstract.** Steel suspension members subjected to tension and bending offer an economical and efficient alternative for many structural problems. This paper is concerned with the elastic and elastic-plastic behaviour of suspension members with bending stiffness subjected to vertical point and uniformly distributed loads. An experimental study is described which focuses on the response of three suspension members with various T-shaped steel hot rolled sections and geometric configurations. The tests enable direct assessment of the influence of a key parameter such as the sag-to-span ratio on the response of suspension members. Detailed nonlinear finite-element models are generated to provide a tool for theoretical analyses and to facilitate further understanding of the behaviour. Results demonstrate that experimentally obtained responses can generally be closely predicted numerically because there are relatively good agreements between finite element and tests results. The results and observations of subsequent numerical parametric studies offer an insight into the key factors that govern the behaviour of suspension members with bending stiffness in the elastic-plastic range.

**Keywords:** steel suspension member with bending stiffness; tests; numerical modelling; finite element nonlinear analysis; elastic-plastic behaviour; mechanism of deformation; analytical solution.

---

## 1. Introduction

Steel suspension members subjected to tension and bending offer an economical and efficient alternative for many structural problems. They can be widely used in bridge and structural engineering and building practice as bearing suspension systems for pedestrian and pipeline bridges as well as for large-span roofs and floors in buildings.

Using steel suspension members with bending stiffness can be an advantage since they do not need special stabilization to eliminate structural kinematics and are mostly subjected to the tension stress, mainly in the case of symmetric loads, thus stability problems are significantly limited.

There have been a few research results and analytical studies published on non-linear solutions of suspension members with bending stiffness and parabolic or similar profile.

Otto (1973) provided an extensive review on the state of the art tension structures and he with his co-workers conducted extensive research on structural form and behaviour of lightweight suspension structures.

Vedenikov and Teloyan (1977) derived closed-form analytical model for geometrically non-linear and

---

\* Corresponding author, Professor, E-mail: [stanislav.kmet@tuke.sk](mailto:stanislav.kmet@tuke.sk)

materially linear suspension members with bending stiffness loaded by various types of continuous and discrete load. Moskalev (1980) solved one time statically indeterminate elastic problem by means of the force method considering elastic yielding of supports. These theories provide simple methods for finding the static response of a hinge-suspension member to applied vertical loads in the elastic range.

Comprehensive analytical treatments on the behaviour of suspension members with ultimate bending stiffness in the elastic-plastic range have been given by Skladnev and Shimanovsky (1992). They proposed a closed-form solution for geometrically and materially non-linear suspension members with bending stiffness and presented some numerical results. Numerical studies with a different bending stiffness of suspension members show that the members with larger stiffness are more deformable than the members with less stiffness. The latter, in turn, reach the full plasticity phase faster and in their behaviour become similar to flexible tendons.

Because of mathematical derivation difficulties that can arise in a geometrically and parametrically non-linear analytical solution, numerical methods are by far the most popular. Most of the recent methods of non-linear analysis of suspension structures are based on the discretisation of the equilibrium equations using FEM and solving the resulting non-linear algebraic equations by numerical methods (Kmet and Bin 2002).

Experimental and theoretical investigation of the three-hinge suspension structure with final bending stiffness made of the two straight-line concrete-filled steel circular tubular members has been conducted by Kvedaras and Sharashkinas (2003). Assessment of behaviour of the composite hollow concrete-filled steel tubular members under tension and bending and closed-form methods for their analysis were performed.

Kmet *et al.* (2006) used a geometrically non-linear closed-form static solution and elastic-plastic design method (determination of internal forces in the elastic range and utilization of critical sections in the plastic range) for a probabilistic simulation-based reliability assessment of the large-span suspension members with bending stiffness under a randomly distributed symmetric and asymmetric load.

Farkas and Jarmai (2008) presented optimization procedure of large-span suspension steel members made of rolled I-sections. In the optimization process the systematic search determines the optimal rolled I-section suspension member with bending stiffness for a numerical problem, which fulfills the constraints on plastic stress, lateral torsional buckling and deflection for asymmetric load and its cross-sectional area as the objective function is minimal. Parametric investigations showed the effect of span length and the initial mid-span sag on the optimum cross section values. Lacarbonara and Pacitti (2008) assessed the influence of the flexural stiffness on the nonlinear static responses of tension members.

Suspension steel members with bending stiffness represent an addition to the range of suspension cable structures available to structural engineers. However, despite interest in their application on the basis of both architectural appeal and structural efficiency, a lack of verified analytical approaches and design guidance is inhibiting uptake. Even though, some authors present the experimentally obtained results of the special elastic-plastic behaviour problems and others investigate the influence of the bending stiffness of tensioned members in general terms theoretically, compare various models and data or study specific aspects through numerical experiments (Tesar and Lago 2009). Rosen and Gur (2009) described a nonlinear transfer matrix model of curved and pretwisted rods, which is capable of analyzing very large spatial deformations. Ozkan and Mohareb (2009) presented the study aimed at determining whether the steel pipes are able to attain their modified plastic moment as predicted by analytically derived plastic interaction relations. The moment versus curvature relations and peak moment values of the specimens as obtained from the experiments are documented. Hijmissen *et al.* (2009) investigated the effect of the bending stiffness on the damping properties of a tensioned member.

Kiyamaz (2009) investigated the bearing strength of stainless steel bolted plates under in-plane tension. Peng *et al.* (2011) presented the complex variable element-free Galerkin method for two-dimensional elasto-plasticity problems. Goldfeld (2009) presented a direct identification procedure for assessment of the stiffness distribution in structures. This procedure is applicable to a variety of structure types, including frames, beams and trusses. Da Silva and Beck (2011) developed the Chaos-Galerkin scheme as the efficient method for the solution of stochastic bending problems in engineering.

Sousa *et al.* (2011) analyzed the influence of bending and shear stiffness in vibrations of cables. Jing and Li (2011) analyzed the effect of the bending stiffness of cables on stress distribution and curve shape in super-long single suspension cable structures. Xia and Cai (2011) derived the equivalent stiffness method to analyze the sag effect of stay cables in cable-stayed bridges.

Currently, few experimental and theoretical results on suspension steel members with bending stiffness exist and there is a limited understanding of their real behaviour in the elastic-plastic and plastic range. Therefore, the purpose of this paper is to improve knowledge about the elastic and elastic-plastic behaviour of suspension members with bending stiffness. The generation of their computational models and structural response data through the results of laboratory testing and numerical modelling and parametric studies upon which nonlinear analysis and structural design may be performed are presented.

The paper presents basic results obtained from the experimental and theoretical research performed on the elastic and elastic-plastic range of suspension steel members with bending stiffness during the process of their loading.

## **2. Laboratory testing**

Recent experimental program on behaviour of suspension members with bending stiffness has been conducted at the Bearing Structures Laboratory in the Institute of Structural Engineering of the Faculty of Civil Engineering at Technical University in Kosice; the testing results of these studies are described herein.

### *2.1 Suspension member tests*

A total of three suspension steel members with bending stiffness were tested in the elastic-plastic range (the size of the plastic range was limited due to the safety) to investigate behaviour and to assess load carrying capacity and deformation capacity. Suspension members were tested in the purpose-built test rigid frames with anchored tension bars for supporting the specimens. The distance between the frames and/or the selection of suspension members' spans was limited largely by spatial possibilities of the laboratory hall. Span of approximately 14 m and two section sizes were selected for suspension members tested. The general layout of the tests is illustrated in Fig. 1. For each member three material tensile coupon tests were conducted.

#### *2.1.1 Suspension member specimens*

The experimental research program included the testing of three steel suspension member specimens with bending stiffness having homogenous cross-sections with different profile geometry (three different sag-to-span ratios were considered) and dimensions. All test specimens were hot rolled members with T cross-section, designed according to the Eurocode 3 (EN 1993-1-1 2005). The geometry of the T sections tested is shown in Fig. 2. Annealing process to relieve residual stresses in the hot rolled steel



Fig. 1 General layout of the test

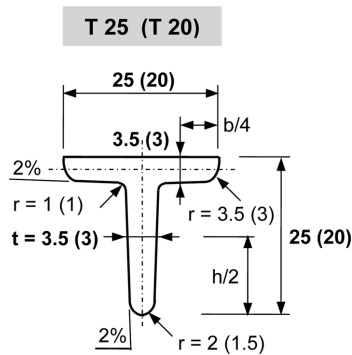


Fig. 2 The basic geometry of the T sections tested

members was not applied. Consequently, the steel members were not stress relieved before the tests.

Table 1 presents total research program, designed geometrical dimensions and material of the individual test members, their span and sag, and span-to-sag ratios. The steel used is *S* 235 with guaranteed yielding stress of 235 MPa and tensile strength of 360 MPa. Dimensions of the suspension T members before deformation are shown in Fig. 3. Test members were made from one piece without mutual connections. Both ends of specimens were ended by pin joint terminals (pin hinges). Pin connecting plates were welded to the end plates of the T members as is shown in Fig. 4.

The suspension members were tested under tension and bending in a 14-point-loading arrangement, to study strains (stresses) and vertical deflections in selected parts between the loading points. The same magnitude loads were applied to the selected points (symmetric discrete loading).

Table 1 Characteristics of suspension members

Member number (-)	Profile (mm)	Steel (-)	Span $l$ (m)	Initial sag $f$ (m)	$l/f$ (-)
1	T 25-1	S 235	14,130	1,295	11
2	T 25-2	S 235	14,130	1,085	13
3	T 20	S 235	14,170	0,980	14,5

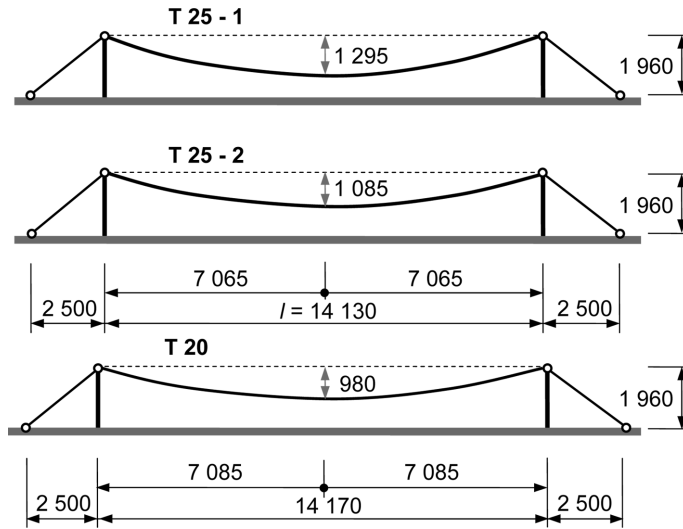


Fig. 3 Dimensions of the suspension T members before deformation

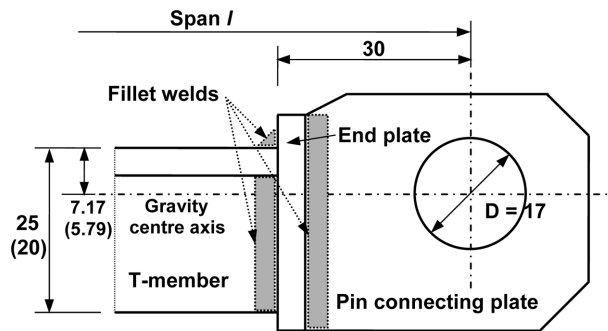


Fig. 4 Scheme of the pinned connection

Prior to testing, measurements of the real geometry of the profile including initial geometric imperfections were performed. Measurements of initial geometric profiles, i.e., initial sag curves of suspension member specimens were important in aiding the explanation of structural response and in the development of numerical models. Therefore a detailed geometric measuring of the characteristic point coordinates of sag curves of the all test suspension members was done before the test and actual values of measured geometries obtained were considered in the further analysis.

### 2.1.2 Test set-up

Special experimental equipment was designed for a realization of tests. This equipment consists of the two opposite anchored steel frames with the required stiffness, global stability and geometry. Frames are anchored to the ground by steel tension rods. A suitable height of the frames enabled an arrangement of the specimens with required sags and at the same time a situation of loading forces. Specially arranged ends of suspension specimen members were connected to the frames by the hinge joints at the same levels.



Table 2 Mean results from tensile coupon tests

Modulus of elasticity $E$ ( $\text{Nmm}^{-2}$ )	Yield stress $f_y$ ( $\text{Nmm}^{-2}$ )	Ultimate tensile stress $f_u$ ( $\text{Nmm}^{-2}$ )
210000	246	386

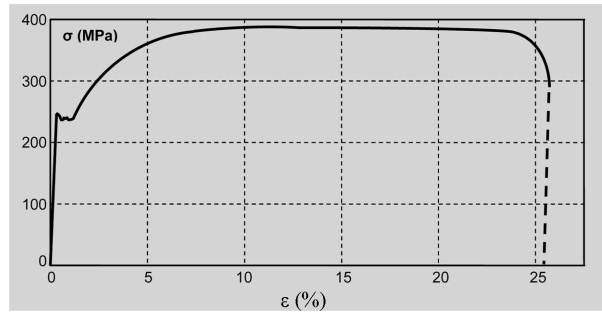


Fig. 6 The characteristic stress-strain diagram

(from flanges  $f_{yf}$  and from webs  $f_{yw}$ ) are higher than the normative values (Kala *et al.* 2009). In all cases of test specimens a good material ductility was also found ( $A_5 > 29\%$ ).

### 2.3 Suspension member results and discussion

The tests of all suspension members were conducted using the methodology mentioned above. In dependence on the sequential load increasing the deflections  $w$  and the strains  $\epsilon$  of the tested members were recorded. Tests revealed the real behaviour of suspension members in the elastic and elastic-plastic range.

Vertical deflections  $w$  in the characteristic areas (positions I3 in the middle of the span and I2 in the quarter of the span of test members as shown in Fig. 5) of the individual test suspension members T 25-1, T 25-2 and T 20 for the applied load levels (loading forces) are shown in Fig. 7. Fig. 7 illustrates the influence of the initial sag on vertical deflections recorded in the middle and in the quarter of the span of test suspension members. Looking at the direct comparison of the deflections shown in Fig. 7 it is clearly visible that maximal elastic and elastic-plastic deflections of suspension members occur in the middle of their span. Elastic and elastic-plastic deflections decrease when the initial sag of the suspension members increases. For tested suspension members the maximal vertical deflections in the middle of the span are:  $w_{3max} = 63,1$  mm (a span-to-deflection ratio is 225) for the T 25-1 member,  $w_{3max} = 75,6$  mm (187) for the T 25-2 member and  $w_{3max} = 86,9$  mm (163) for the T 20 member. Deflections of the test suspension members indicate characteristics associated with the geometrically non-linear behaviour.

Strains and stresses of suspension members were investigated in the areas between the imposed discrete loading forces. Normal stresses at the top and bottom fibres of a cross-section are shown for the characteristic places (positions T1, T2 and T3 as is shown in Fig. 5) of suspension members in Fig. 8 (member T 25-2) and in Fig. 9 (member T 20). Figs. 8 and 9 show that stresses at the bottom fibres are smaller than those at the top fibres of the cross-sections situated in the middle between the loading forces. In both cases the fibres are loaded by tension. It can be explained by the bending moment influence with the opposite direction occurring in the area in the middle between the loading forces

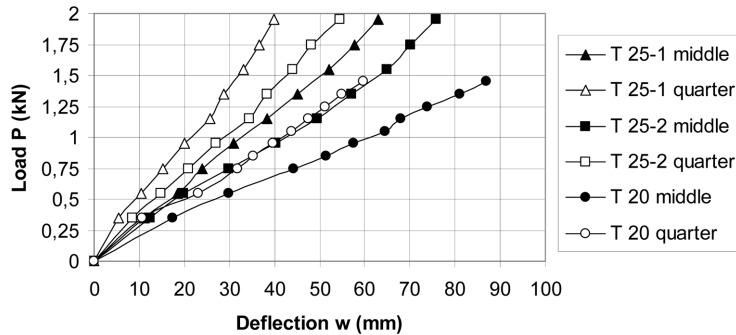


Fig. 7 Comparison of vertical deflections in the middle and quarter of the span of suspension members T 25-1, T 25-2 and T 20

acting as fictitious supports for suspension members (top fibres occurring in the mentioned area are tensioned from the bending moment and the resultant tensile stress is increased). The phenomenon described is typical for the suspension members under the discrete loading conditions while in the case of the continuously distributed load this phenomenon does not occur. However, maximal tensile stresses at the bottom fibres are occurring directly under the loading forces (it will be shown by the numerical experiments because the stresses direct under the loading forces were not possible to measure during the tests) and are bigger than those at the top fibres. Tests demonstrated that suspension members' stresses decrease with increase of initial sag. Behaviour of the tested suspension members is characterised by the tension stress which enables a larger utilization of steel cross-sections since the load carrying capacity of these members (such as the test members) is determined on the basis of strength criterion and not the stability one. Distribution of stresses along the members' span is relatively uniform and no significant extremes occur in the elastic and elastic-plastic range (except local maxima under the loading forces).

Figs. 8 and 9 show that in all cases the maximal tension stresses occur near the hinge supports and are the same at the top and bottom fibres of cross-sections (stress from the bending equals zero). Suspension member T 25-1 did not reach the yield stress  $f_y = 246$  MPa and its behaviour is in the elastic range. Stresses of members T 25-2 and T 20 are beyond the yield stress and their behaviour was influenced by the local plastic zones. Plastic strains provoke the increase of vertical deflections in the middle of the span and also in the quarter of the span of both suspension members. Suspension member T 25-2 reached elastic-plastic behaviour under the loading force  $P = 1,75$  kN (see Fig. 8) and a member T-20 with the smaller cross-section under the loading force  $P = 1,25$  kN (see Fig. 9). After the beginning of elastic-plastic behaviour the stresses in the side fibres of cross sections did not rapidly increase because the plastic strains (and same the plastic stresses) were increased towards the cross-sections' inside. The elastic-plastic behaviour of the member T 20 indicates that stresses in the middle of the span at the bottom fibres begin to near those at the top fibres (it is clear from Fig. 9) and consequently the influence of bending stiffness is decreased when the plastic zone in the sections around the mid-span of the suspension member arises. After the suspension member reaches the phase of full material plasticity (formation and development of plastic zones), its behaviour transforms and becomes similar to behaviour of a suspension cable with the dominant tension stiffness.

Tests showed required load bearing capacity of the investigated suspension members under the stresses beyond the elastic limit: stresses beyond 300 MPa. Under these stresses no failures of the

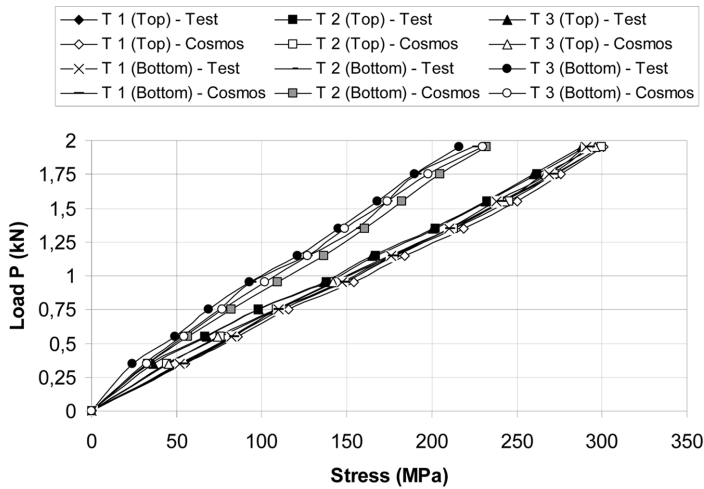


Fig. 8 Experimentally and theoretically obtained stresses at the top and bottom fibres of sections in the middle, quarter and near the support of the test suspension member T 25-2

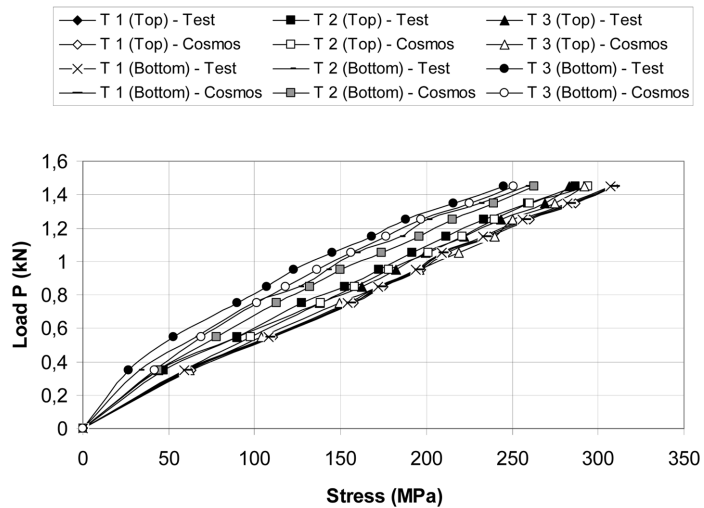


Fig. 9 Experimentally and theoretically obtained stresses at the top and bottom fibres of sections in the middle, quarter and near the support of the test suspension member T 20

suspension members tested were indicated.

### 3. Numerical modelling

A numerical modelling programme was carried out in parallel with the experimental programme. The initial aim of numerical work was to replicate the experimental elastic and elastic-plastic behaviour of suspension members numerically. Subsequent studies were performed to investigate the behaviour and

sensitivity of the models to variation in the key input parameters. All numerical modelling was performed using the non-linear finite element analysis package COSMOS/M version (COSMOS/M 2002).

### 3.1 Generation of the finite element models

The elements chosen for the finite element models were 4-noded shell elements with six degrees of freedom per node (three translations and three rotations), designated as SHELL4T in the COSMOS/M element library. SHELL4T is a quadrilateral thick shell element with membrane and bending capabilities for the analysis of three dimensional structural models. The element accounts for shear deformation effects (the Mindlin plate theory is applied). The element is assumed to be isotropic with constant thickness. SHELL4T elements with options for large displacements, small plastic strains, the Huber - Hencky - von Mises yield criterion and kinematic hardening are used in the analyses.

This element has been shown to perform well in similar applications involving the modelling of stainless steel bending members. Convergence studies were conducted to decide upon an appropriate mesh density, with the aim of achieving suitably accurate results whilst minimising computational time. Meshes with dimensions of 4×3 mm were used as shown in Fig. 10.

The incremental method with Newton-Raphson iterative procedures was employed to solve the geometrically and materially non-linear suspension member model. Ten increments of the loading forces with twenty iterations for each loading increment were considered. The plastic zones method applied enables effective solutions to be found to plastic strains across the cross-section and/or along the sag curve of suspension members and adequately modifies their stiffness.

### 3.2 Material modelling

Material behaviour was specified by means of a real stress-strain curve, defined in terms of engineering stress and strain. The measured average material properties (such as the Young's modulus and yield stress) taken from tensile coupon tests were adopted in all cases. This was deemed acceptable since there was little variation in material properties among specimens. Approximation of the stress-strain curve used in studies is given in Fig. 11. The elastic-plastic material model with the strain hardening (with the corresponding strain hardening moduli:  $E_{h1} = 3600$  MPa and  $E_{h2} = 2500$  MPa) is considered. Residual stresses were not incorporated in the finite element models in this study.

### 3.3 Geometry modelling

For the suspension member models actual geometries of the profiles (sag curves) were included in the

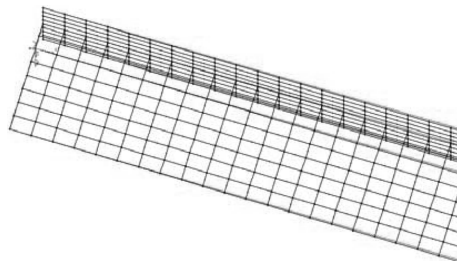


Fig. 10 3D model with appropriate mesh density

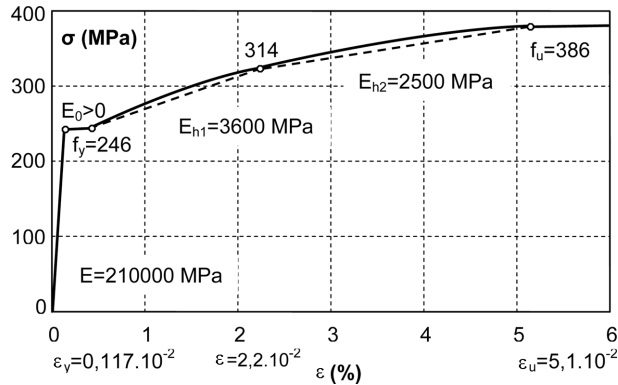


Fig. 11 Approximation of the real stress-strain curve

non-linear analysis. For the models of individual suspension members actual geometries obtained by the measurement of characteristic nodal coordinates of their sag curves were used. Global geometric imperfections in comparison with ideal parabolic profiles were carefully measured and individual imperfections of nodal coordinates (in all three directions) were obtained for the initial state when members were loaded by their self weight only (including the weight of installed barrels).

### 3.4 Simulation of tests and discussion of the results

The suspension member tests were modelled using the applied loading forces from the tests, material stress-strain data from the corresponding tensile tests and actual geometric properties of the suspension member profile (a sag-curve form). Displacements of supports in the horizontal direction were considered at the individual load levels. The corresponding boundary conditions were applied to model hinge end supports.

Behaviour (mechanism of deformation) of the suspension member T 25-2 with local deformations in the positions under the discrete loading forces and between the loading forces (with the upward direction) is shown in Fig. 12 (graphical output from COSMOS/M software). Detail of the suspension

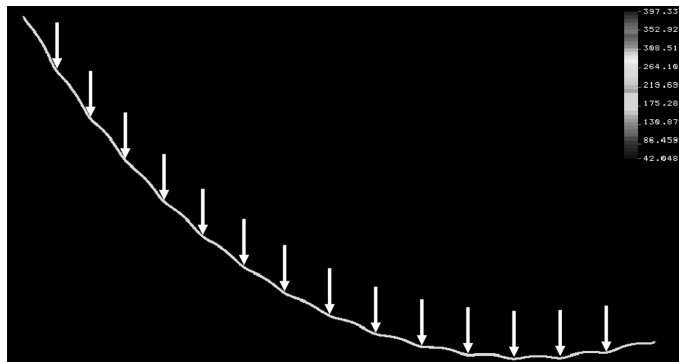


Fig. 12 Behaviour (mechanism of deformation) of the suspension member T 25-2 with local deformations in the positions under the discrete loading forces and between the loading forces (with the upward direction)

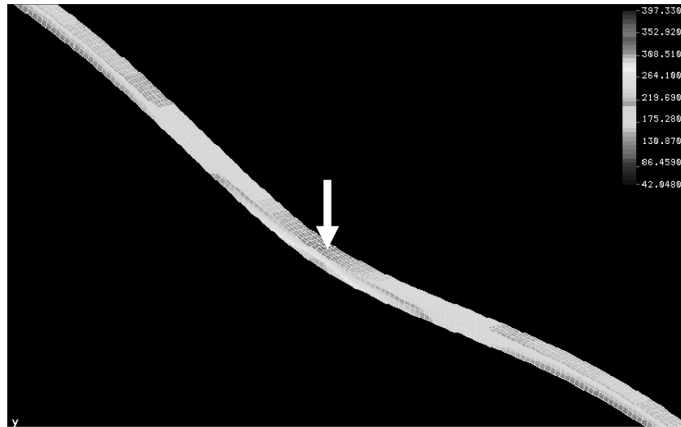


Fig. 13 Detail of the local deformation of the suspension member in the position under the discrete loading force (maximal tension stress at the bottom fibres) and between the loading forces with the up-ward directions on the left-hand and right-hand side (maximal tension stress at the top fibres)

member local deformation in the position under the discrete loading force (maximal tension stress at the bottom fibres) and between the loading forces with the up-ward directions on the left-hand and right-hand side (maximal tension stress at the top fibres) is shown in Fig. 13.

Distributions of stresses along cross-sections of the suspension member in the zone under the loading force and in the zone between the loading forces in the middle of the span and in the quarter of the span are illustrated, for the suspension member T 25-2 and the 7<sup>th</sup> loading state (LS), in Fig. 14 (graphical output from COSMOS/M software).

On the basis of the analysis of stress distributions along cross-sections of suspension members in the zones between the loading forces and in the zone under a loading force as is shown in Fig. 14, the following observations can be made: in the area between the discrete loading forces the maximum stresses occur at the top fibres of cross-sections, while in the area under the discrete loading forces the maximum stresses occur at the bottom fibres of cross-sections. These numerical results were confirmed by the results obtained from the tests as is clear from Fig. 8 for the T 25-2 suspension member and/or from Fig. 9 for the T 20 suspension member. Theoretically obtained behaviour of suspension members confirmed the obtained tests' results.

Comparison of the vertical deflections in the middle of the span of suspension members T 25-1, T 25-2 and T 20 obtained by the tests and those obtained by the COSMOS/M software is shown in Fig. 15. A comparison of the vertical deflections in the quarter of the span of suspension members T 25-1, T 25-2 and T 20 obtained by the tests and those obtained by the COSMOS/M software is shown in Fig. 16. The relative differences between the theoretical and experimental values of deflections are not too big and have a tendency of reduction with the growing loading forces. Greatest differences between the theoretically and experimentally obtained deflections were received at the beginning of the tests: about 20%. With an increasing of the loading forces this difference decreased to about 4%. The greatest differences among theoretically and experimentally obtained stresses at the beginning of the tests were about 22% and with increasing of the loading forces these differences decreased to about 3-11% (Figs. 8 and 9).

The levels of bending stresses at top and bottom fibres depend on the size of sections of suspension members and on the investigated positions as are positions between the loading forces or under the

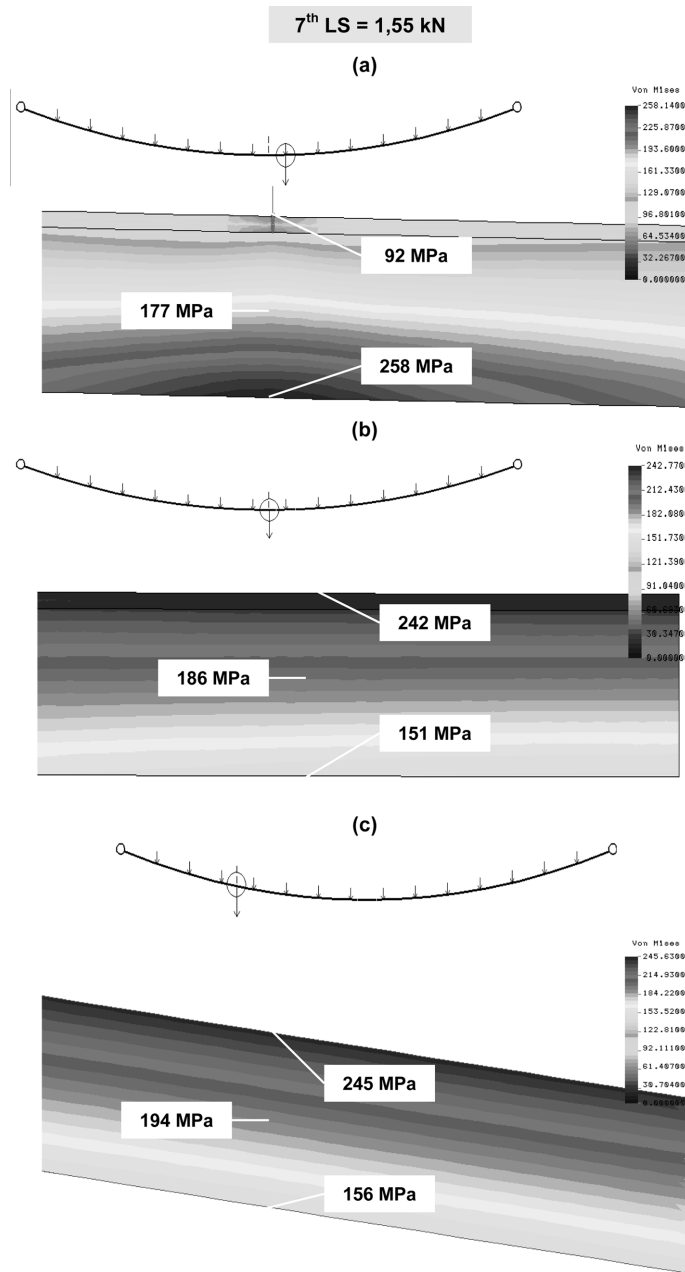


Fig. 14 Distribution of stresses along cross-sections of the suspension member in the zone under the loading force (a), and in the zone between the loading forces in the middle of the span (b) and in the quarter of the span (c), for the suspension member T 25-2 and the 7<sup>th</sup> loading state, (graphical output from *COSMOS/M* software)

loading forces, positions at the middle of the span or at the quarter, etc. The bending stiffness of the suspension members and the type of their load (a discrete or distributed load), have an overriding

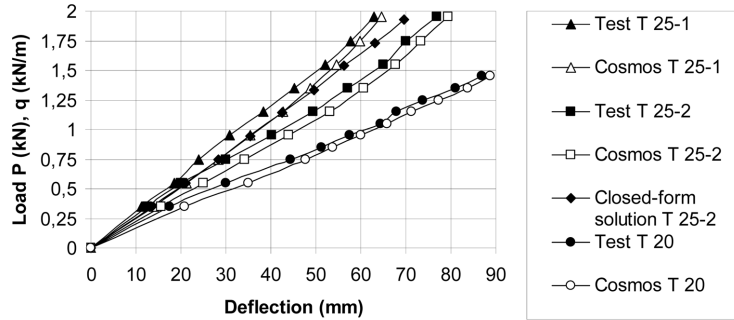


Fig. 15 Comparison of the vertical deflections in the middle of the span of suspension members T 25-1, T 25-2 and T 20 obtained by tests and those obtained by COSMOS/M software and by closed-form solution for the T 25-2 member

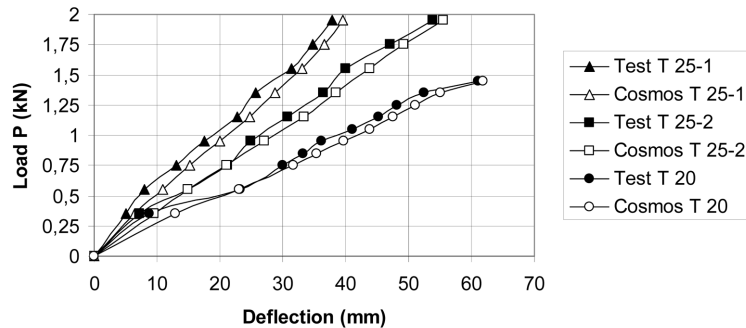


Fig. 16 Comparison of the vertical deflections in the quarter of the span of suspension members T 25-1, T 25-2 and T 20 obtained by tests and those obtained by COSMOS/M software

influence on their behaviour and/or on the level and distribution of bending and axial tension stresses. The percentage values of the level of bending stresses in regard of the level of axial tension stresses vary, depending on the load and position, as follows. For the T 25-2 member the level of bending stresses at the cross-sections situated between the loading forces at the middle of the span (at the quarter of the span) vary from 7,8% to 9,4% (from 6,9% to 9,2%) at top fibres and from -18,2% to -23,1% (from -16,4% to -19,5%) at bottom fibres. For the T 20 member the level of bending stresses at the cross-sections situated between the loading forces at the middle of the span (at the quarter of the span) vary from 6,2% to 13,8% (from 2,1% to 8,5%) at top fibres and from -15,9% to -27,1% (from -5,7% to -17,3%) at bottom fibres. The levels of elastic bending stresses at the cross-sections situated under the loading forces are substantially higher due to the local bending (about -45% at the top fibres and 80% at the bottom fibres for the T 25-2 member and about -30% at the top fibres and 75% at the bottom fibres for the T 20 member).

Figs. 8, 9, 15 and 16 demonstrate that test response can generally be closely predicted numerically because there are relatively good agreements between finite element and tests' results. Theoretically obtained results are in majority of cases larger than the values obtained experimentally. Some differences in the results could be caused by local stresses due to the connection of discrete loads.

Results confirmed physical relevance and logical correctness of the applied theoretical approach.

#### 4. Comparison of results obtained by closed-form solution

In order to compare results obtained by tests and finite element analysis, when COSMOS/M software is used, with those obtained by a closed-form solution developed by Vedenikov and Teloyan (1977), solutions in the elastic range have been generated for the suspension member with bending stiffness under a vertical uniformly distributed load  $q$  applied over the entire span of the steel member.

##### 4.1 Brief description of the closed-form solution

Basic scheme for the materially linear (elastic range) and geometrically nonlinear closed-form static solution of suspension members with bending stiffness and the parabolic profile defined as

$$z_0(x) = \frac{4d_0}{l^2}x(l-x) \tag{1}$$

where  $d_0$  is the sag in the middle of the span  $l$  of the member under its self weight  $g$  is shown in Fig. 17. The closed-form solution presented is based on the following underlying assumptions: The profile of a member hanging under its own weight between two supports is flat, so that the ratio of sag to span is 1:8 or less. This profile can be approximated by quadratic parabola and specified by Eq. (1). This corresponds to the situation where suspension members with relatively low sags were investigated. The member is homogeneous with a constant cross section along its entire length. Only a vertical uniformly distributed static load is considered in the solution. More details on the formulation can be found in reference Vedenikov and Teloyan (1977). The discrete loading forces generated for the suspension members during the tests were transformed into the equivalent uniformly distributed load. This creates not the totally same loading conditions particularly in this case of suspension members, and consequently, the resultant action effects can be a bit different.

The following cubic equation for vertical deflection  $w$  in the middle of the span  $l$  of the suspension member under a uniformly distributed load  $q = g + p$  ( $g$  is the permanent load and  $p$  is the variable load) applied over the entire span of the suspension member (symmetric loading) with flexible supports in the horizontal direction was derived by Vedenikov and Teloyan (1977)

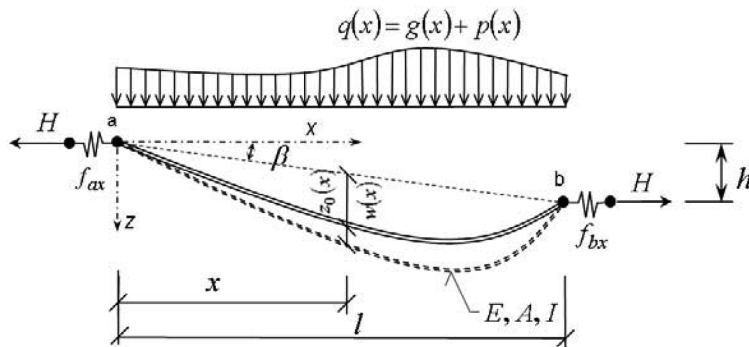


Fig. 17 Basic scheme, geometry and loading of suspension member with bending stiffness

$$C_1 w^3 + C_2 w^2 + C_3 w - C_4 = 0 \quad (2)$$

with the coefficients  $C_1$ ,  $C_2$ ,  $C_3$  and  $C_4$  in the form

$$C_1 = \frac{4 c A}{15 c_L I}, \quad C_2 = \frac{4 c A}{5 c_L I} d_0,$$

$$C_3 = \frac{8 c A}{15 c_L I} d_0^2 + \frac{1}{80} \frac{g l^4}{E I d_0} + 1, \quad (3)$$

$$C_4 = \frac{1}{80} \frac{p l^4}{E I}$$

where  $A$  is the cross-sectional area of the suspension member,  $I$  is the second moment of area and  $E$  is the Young's modulus of the suspension member with bending stiffness.

The coefficient of supports flexibilities  $c$  is given as

$$c = \frac{\cos^2 \beta}{1 \pm \frac{E A}{c_L I} (f_{ax} + f_{bx})} \quad (4)$$

where  $f_{ax}$  and  $f_{bx}$  are elastic flexibilities of the support  $a$  and  $b$  in the horizontal direction  $x$ , respectively,  $\beta$  is the inclination of the connecting line of supporting points of the suspension member with the horizontal axis  $x$  (for this case  $\beta = 0$ ). The positive sign in the expression (4) corresponds to the supports displacements in the direction inside of the suspension member span. The coefficient  $c_L$  of the suspension member length is

$$c_L = 1 + \frac{16 d_0^2}{3 l^2} + \tan^2 \beta \quad (5)$$

#### 4.2 Numerical results and discussion

The suspension steel member analyzed was the test member T 25 (the specimen number 2 as is designated in Table 1) with a span  $l = 14130$  mm and initial sag in the middle of the span  $d_0 = 1085$  mm. Input data for the T25 cross-section are:  $A = 164$  mm<sup>2</sup>,  $I = I_y = 8620$  mm<sup>4</sup> and  $E = 210000$  Nmm<sup>2</sup>. Permanent load as a self weight of the member is  $g = 0,0128$  Nmm<sup>-1</sup>. Vertical deflections in the middle of the span of the suspension member were investigated under the vertical uniformly distributed load levels  $q = g + p$  applied over its entire span. The horizontal flexibility of the supporting system in the form of the anchored hinge post was calculated from the expression  $f_{ax} = L_a / E_a A_a \cos^2 \alpha = 0,00014$ , where  $L_a$  is the length of the anchoring member,  $E_a$  is the modulus of elasticity of the anchoring member,  $A_a$  is the cross-sectional area of the anchoring member and  $\alpha$  is the angle formed by the anchoring member with the  $x$ -axis. Substituting support flexibilities  $f_{ax} = f_{bx} = 0,00014$  in Eq. (4) the coefficient of supports flexibilities  $c = 0,6$  is obtained.

Vertical deflections  $w$  in the middle of the suspension member span versus applied loads obtained by the test, by the nonlinear finite element method (where COSMOS/M software with the same approach and generation of the finite element model as in the section 3 was used) and by the present closed-form

solution (when Eq. (2) was used) are shown in Fig. 15. This demonstrates that there are differences between the elastic deflections of the investigated suspension member obtained by the test, finite element method and closed-form solution. These differences increase when the load levels are increased. The greatest difference is 13,2% in the comparison with the test results and 16,7% in the comparison with the finite element results. Deflections obtained by the closed-form solution are less than those obtained by the test and finite element method. The reasons of these differences may be the use of the uniformly distributed load instead of the discrete point load, imperfections in the initial geometric profile, neglect of the influence due to residual stresses and a smaller accuracy of the expression for suspension member length in the closed-form solution.

### 5. Parametric studies: results and discussion

Following the satisfactory agreement between test and finite element model behaviour, this section presents parametric studies, intended to generate a greater pool of results upon which design guidance for suspension steel members with bending stiffness may be based.

The influence of the following parameters was investigated by means of the parametric study on the behaviour of suspension members with bending stiffness in the elastic-plastic region: the size of the initial sag (a sag 3,6 m (with sag-to-span ratio  $f_0/l = 0,06$ ), 6,0 m ( $f_0/l = 0,1$ ) and 9,0 m ( $f_0/l = 0,15$ ) was considered) and the intensity of the continuous uniformly distributed load along the entire span of the suspension member, i.e., symmetric load (elastic and plastic range of loading, behaviour in the elastic and elastic-plastic region was considered). Static scheme, load, geometry and welded I-section characteristics of the studied suspension member with bending stiffness with unmovable supports are shown in Fig. 18. In Fig. 18 is also the following denotation of the investigated points: 1- in the middle of the span, 2- in the third of the span, 3- in the sixth of the span and 4- near the support.

2D beam finite element type BEAM was selected through COSMOS/M software and used for parametric studies. Profile of the suspension member was divided into 300 straight hinge edged finite elements of length approximately 200 mm. Incremental method with Newton-Raphson iterative procedure was used for a solution of the geometrically and materially non-linear problem. Ten increments of load and twenty iterations at each step (load increment) were considered for a solution of the non-linear task. Bi-linear approximation of the stress-strain relation for the elastic-plastic material model with the linear strain hardening (with yield stress  $f_y = 235$  MPa and with the strain hardening modulus:  $E_h = 2800$  MPa) is considered.

Only some of the results and conclusions for the symmetric load are present herein. Values of the normal forces increase at all the sags towards the supports as is shown in Fig. 19. If the sag is increased, normal forces are decreased. In the stage of the elastic-plastic and plastic behaviour of some cross-

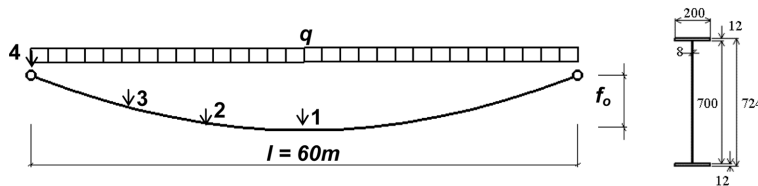


Fig. 18 Static scheme, load, geometry, and welded cross-section characteristic of the studied suspension member with bending stiffness with denotation of investigated points

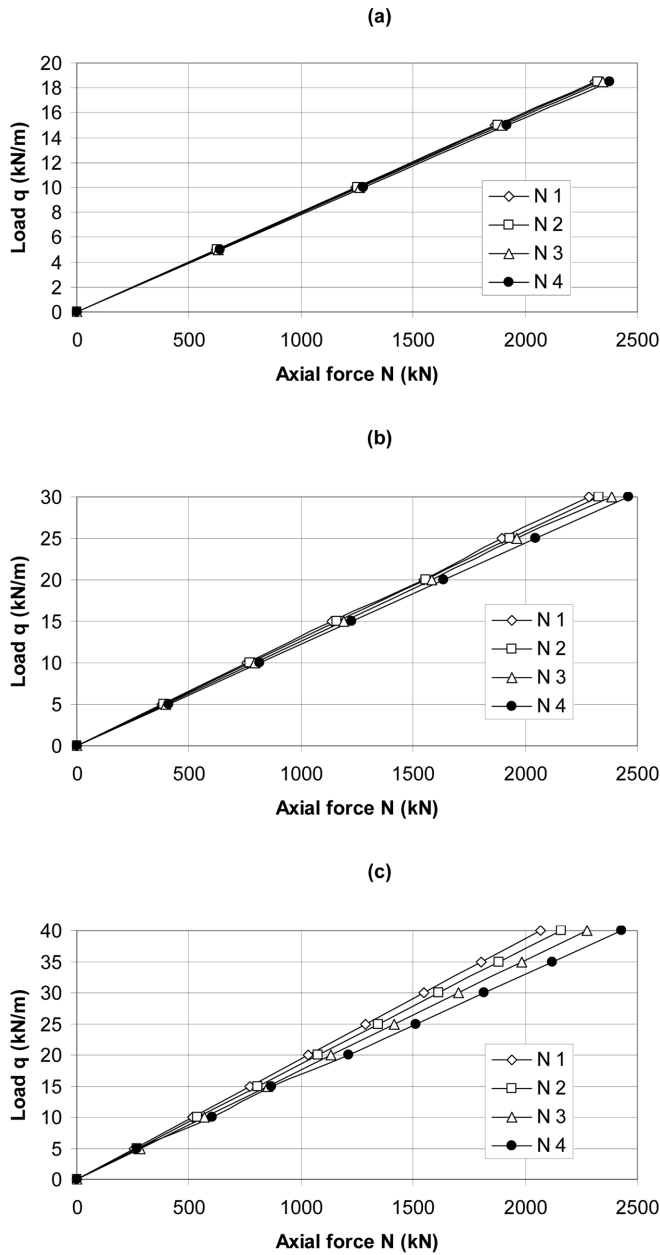


Fig. 19 Normal forces in cross-sections 1, 2, 3 and 4 of the suspension member with bending stiffness with the initial sag in the middle of span  $f_0 = 3,6$  m (a),  $f_0 = 6,0$  m (b) and  $f_0 = 9,0$  m (c) versus corresponding load levels

sections in the middle of the span and at its neighbourhood bending moments of the individual suspension members begin rapidly decrease as shown in Fig. 20(a) at the load level  $q = 15 \text{ kNm}^{-1}$  (then an origin of the plastic hinge occurred) for the member with an initial sag  $f_0 = 3,6$  m, in Fig. 20(b) at the load  $q = 25 \text{ kNm}^{-1}$  (origin of the plastic hinge) for the member with an initial sag  $f_0 = 6,0$  m and finally

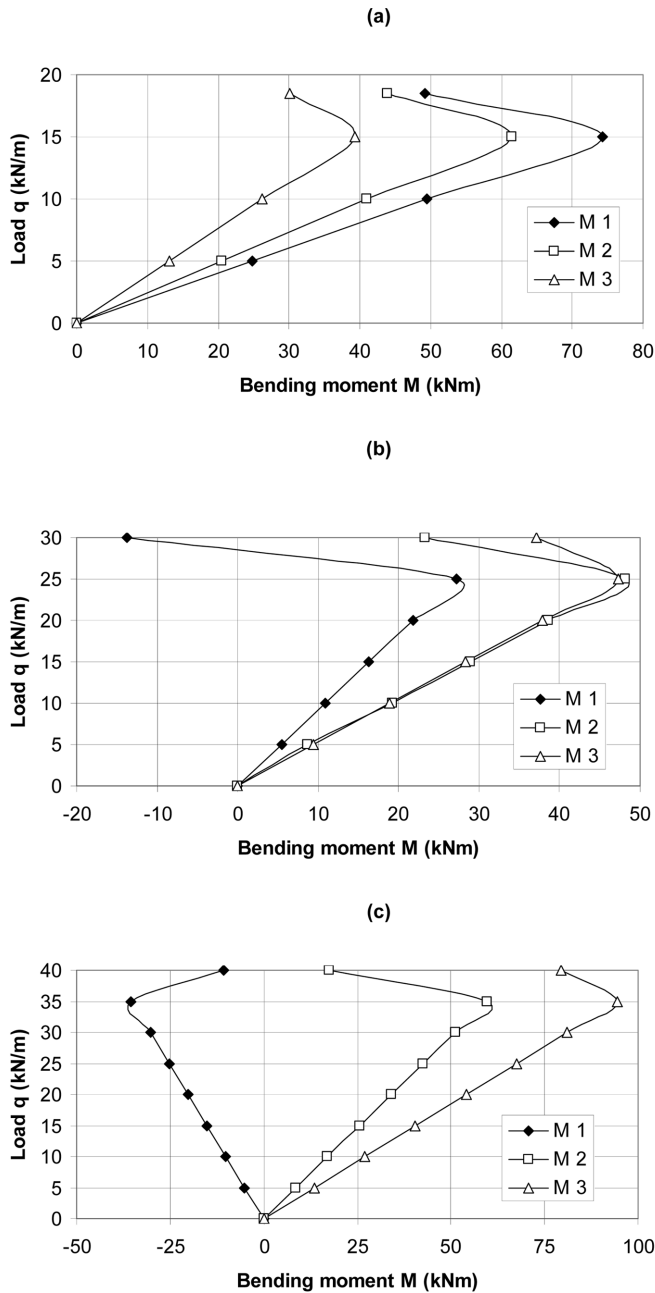


Fig. 20 Bending moments in cross-sections 1, 2 and 3 of the suspension member with bending stiffness with the initial sag in the middle of span  $f_0 = 3,6 \text{ m}$  (a),  $f_0 = 6,0 \text{ m}$  (b) and  $f_0 = 9,0 \text{ m}$  (c) versus corresponding load levels

in Fig. 20(c) at the load  $q = 35 \text{ kNm}^{-1}$  (origin of the plastic hinge) for the member with an initial sag  $f_0 = 9,0 \text{ m}$ . This is the state of transformation of the suspension member with bending stiffness into the suspension member with the dominant axial tension stiffness (with a similar behaviour to the suspension

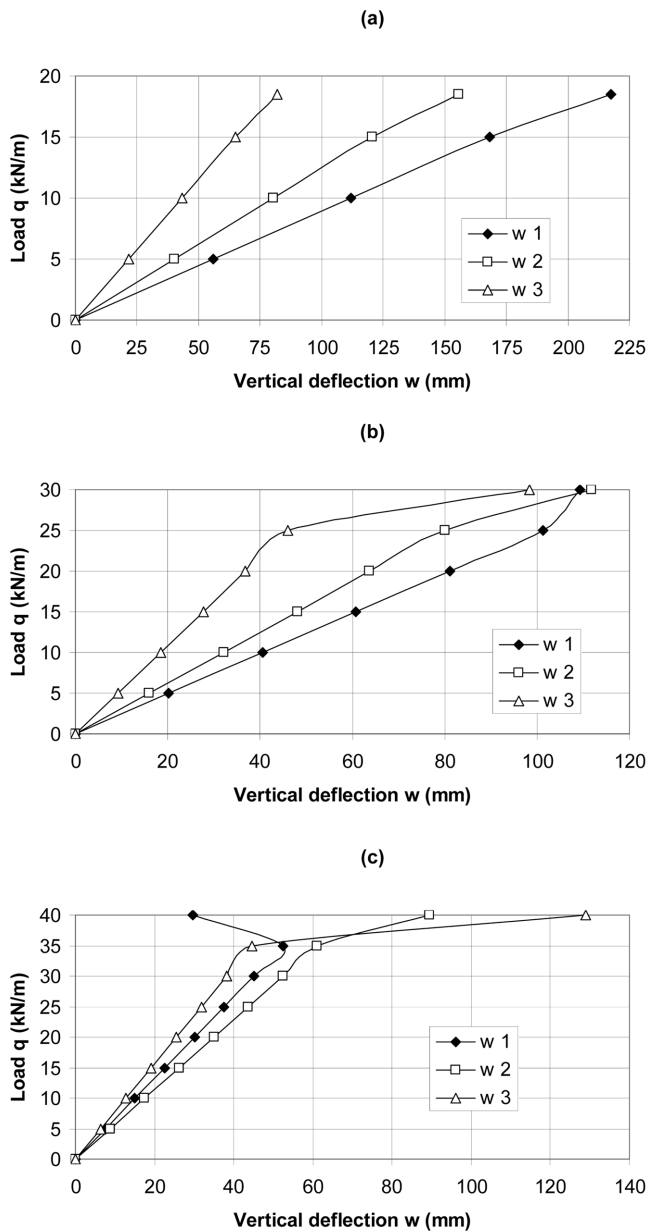


Fig. 21 Vertical deflections in places 1, 2 and 3 of the suspension member with bending stiffness with the initial sag in the middle of span  $f_0 = 3,6$  m (a),  $f_0 = 6,0$  m (b) and  $f_0 = 9,0$  m (c) versus corresponding load levels

cables). This is the reason why in the plastic region one can denote these suspension members as suspension members with final bending stiffness. Increase of the initial sag decreases normal stresses in the cross-sections of the suspension members.

When normal stresses overcome the yield stress deflections in the middle of the span and in its neighbourhood begin to decrease and on the other hand deflections in the third and sixth of the span

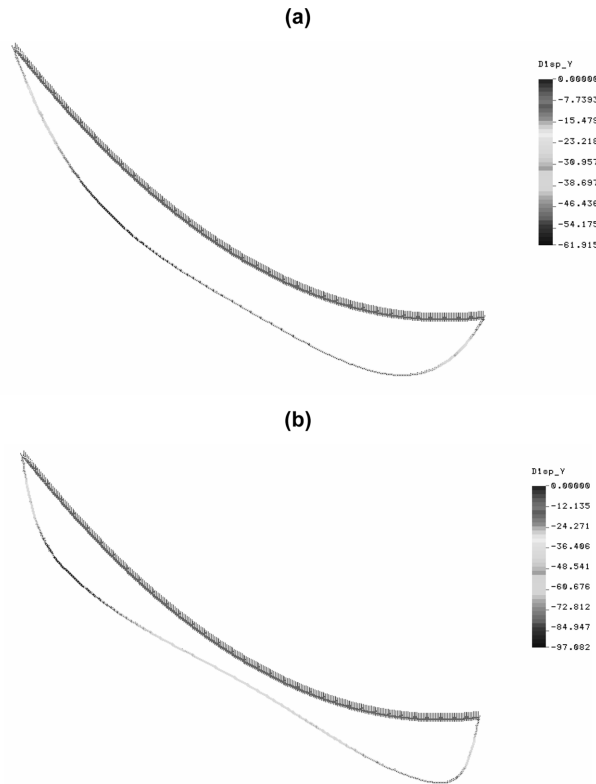


Fig. 22 Deflection curve of the suspension member with bending stiffness with the initial sag in the middle of span  $f_0 = 9,0$  m (graphical output of COSMOS/M software): under the load  $q = 35 \text{ kNm}^{-1}$  (a) and  $q = 40 \text{ kNm}^{-1}$  (b)

begin to increase rapidly, and they are already larger than those in the middle of the span as is clear from Fig. 21(b) and Fig. 21(c). In the case of the suspension member with a small initial sag  $f_0 = 3,6$  m all deflections are increased as is shown in Fig. 21(a).

At the elastic-plastic stage a significant redistribution of deflections can occur in the suspension member. Their maximum values are at approximately  $0,15l$  ( $l$  is the span of the suspension member) distance from supports as is clear from Fig. 22 and negative displacements in the middle of the span appear.

Elastic and elastic-plastic behaviour of suspension members with bending stiffness depends in a large scale on the initial geometry of their profiles (on the sag-to-span ratios) and on their stiffness.

## 5. Conclusions

In this paper the results from the experimental and theoretical analysis on the elastic and elastic-plastic behaviour of suspension members with bending stiffness subjected to vertical discrete load and to uniformly distributed load applied over the entire span have been presented.

Behaviour of suspension members in the elastic and elastic-plastic range was investigated by tests

and the obtained results were confirmed by geometrically and materially nonlinear finite element analysis. All numerical modelling was performed using the non-linear finite element analysis package COSMOS/M version. Results demonstrated that test response can generally be closely predicted numerically because there were relatively good agreements between finite element and tests results. Results confirmed physical relevance and logical correctness of the applied theoretical approach.

Subsequent parametric studies were performed to investigate the behaviour and sensitivity of the suspension members to variation in the key input parameters (sag-to-span ratio and size of load in the elastic-plastic range).

Mechanism of deformation was studied and described for the selected types of suspension members during the process of their loading by symmetric loads. The continued effort for economic design of steel structures tends to decrease their weight by shape and material optimization, e.g., through using the suspension members with bending stiffness made from usual structural steels. The efficiency of steel suspension members with bending stiffness is evident in the case of their elastic-plastic behaviour. The growth of plastic deformations provokes the redistribution of stresses and bending moments in the suspension members which often leads to the increase of their bearing capacity and more effective under load behaviour.

The results of presented research affirm and expand the knowledge of previous research about the elastic and elastic-plastic behaviour and load-carrying capacity of suspension members with bending stiffness with steel homogenous cross-sections. Elastic-plastic behaviour and load-carrying capacity of suspension members with bending stiffness depends in a large scale on the initial profile shapes and their later formation and changes during the loading process. Load-carrying capacity of the suspension members with bending stiffness increases by their transformation into the suspension members with mainly tension stiffness during the elastic-plastic and plastic stage of their behaviour.

The applied approach holds a promise in solving more complex analysis of suspension members with bending stiffness. Future work will consider the application of the presented experimental and theoretical methodologies to more complex problems, including the nonlinear analysis of the suspension member behaviour under asymmetric load and non-homogeneous boundary conditions (influence of elastic yielding supports).

It is believed that the approach presented will lead to an improved modelling, analysis and design of suspension members with bending stiffness.

## Acknowledgements

This work is part of the Research project No. 1/0321/12, founded by the Scientific Grant Agency of the Ministry of Education of Slovak Republic and the Slovak Academy of Sciences. The present research has been carried out within the project Centre of excellent integrated research of the progressive building structures, materials and technologies, supported from the Structural funds of the European Union.

## References

- COSMOS/M (2002), "*Version Geostar 2.8*", Structural Research Analysis Centre, Los Angeles.  
Da Silva, C. R. A. and Beck, A. T. (2011), "Chaos-Galerkin solution of stochastic Timoshenko bending problems",

- Comput. Struct.*, **89**(7-8), 599-611.
- EN 1993-1-1 (2005), “*Design of steel structures. General rules and rules for Buildings*”, CEN, Brussels.
- Farkas, J. and Jarmai, K. (2008), “*Design and Optimization of Metal Structures*”, Horwood Publishing, Chichester.
- Goldfeld, Y. (2009), “A direct identification procedure for assessment of stiffness distribution”, *Eng. Struct.*, **31**(5), 1068-1076.
- Hijmissen, J. W., van den Heuvel, N. W. and van Horsen, W. T. (2009), “On the effect of the bending stiffness on the damping properties of a tensioned cable with an attached tuned-mass-damper”, *Eng. Struct.*, **31**(5), 1276-1285.
- ISO 6892-1 (2009), “*Metallic materials - Tensile testing - Part 1: Method of test at room temperature*”, International organization for standardization.
- Jing, T. H. and Li, Q. N. (2011), “Effects analysis of bending stiffness of cables on stress distribution and curve shape in super-long single suspension cable structures”, *Advances Materials Research*, **163**, 173-176.
- Kala, Z., Melcher, J. and Puklicky, L. (2009), “Material and geometrical characteristics of structural steels based on statistical analysis of metallurgical products”, *Journal of Civil Engineering and Management*, **15**(3), 299-307.
- Kiyamaz, G. (2009), “Investigations on the bearing strength of stainless steel bolted plates under in-plane tension”, *Steel Compos. Struct.*, **9**(2), 173-189.
- Kmet, S. and Bin, M. (2002), “Analysis of non-linear suspension members with bending stiffness”, *Struct. Eng.*, **50**(2), 11-17.
- Kmet, S., Jarmai, K., Farkas, J. and Kanocz, J. (2006), “Optimum design and reliability of large-span suspension members”, *Proceedings of the IABSE Symposium on Responding to Tomorrow's Challenges in Structural Engineering*, Budapest, September.
- Kvedaras, A. K. and Sharashkinas, V. (2003), “Behaviour of hollow concrete-filled steel members subjected to tension and bending”, *Proceedings of the International Conference on Metal Structures ICMS-03*, Miskolc, April.
- Lacarbonara, W. and Pacitti, A. (2008), “Nonlinear modeling of cables with flexural stiffness”, *Mathematical Problems in Engineering*, **2008**, 1-21.
- Moskalev, N. S. (1980), “Structures of suspension roofs”, Strojizdat, Moscow, (in Russian).
- Otto, F. (1973), “*Tensile structures: design, structure and calculation of buildings of cables, nets and membranes*”, The MIT Press, Cambridge, Massachusetts.
- Ozkan, I. F. and Mohareb, M. (2009), “Testing and analysis of steel pipes under bending, tension and internal pressure”, *J. Struct. Eng.*, ASCE, **135**(2), 187-197.
- Peng, M., Li, D. and Cheng, Y. (2011), “The complex variable element-free Galerkin (CVEFG) method for elasto-plasticity problems”, *Eng. Struct.*, **33**(1), 127-135.
- Rosen, A. and Gur, O. (2009), “A transfer matrix model of large deformations of curved rods”, *Comput. Struct.*, **87**(7-8), 467-484.
- Skladnev, N. N. and Shimanovsky, A. V. (1992), “General calculation method for suspension structures of large-span buildings and constructions considering plastic properties of materials”, *Proceedings of the IASS - CSCE International Congress on Innovative Large Span Structures: Concept, Design, Construction*, Toronto.
- Sousa, R. A., Souza, R. M., Figueiredo, F. P. and Menezes, I. F. M. (2011), “The influence of bending and shear stiffness and rotational inertia in vibrations of cables: An analytical approach”, *Eng. Struct.*, **33**(3), 689-695.
- Tesar, A. and Lago, J. (2009), “Aeolic and galloping vibrations of overhead line conductors”, *Building Research Journal*, **57**(3-4), 169-183.
- Vedenikov, G. S. and Teloyan, A. L. (1977), “Non-linear computational method of fibres with bending stiffness”, *Strojitelnaja mehanika i rascet sooruzenij*, **6**, 26-30. (in Russian).
- Xia, G. Y. and Cai, C. S. (2011), “Equivalent stiffness method for nonlinear analysis of stay cables”, *Struct. Eng. Mech., An Int'l Journal*, **39**(5), 661-667.